

Real-time public transport service-level monitoring using passive WiFi: a spectral clustering approach for train timetable estimation

Baoyang Song
Ecole Polytechnique
France
baoyang.song@polytechnique.edu

Laura Wynter
IBM Research
Singapore
lwynter@sg.ibm.com

Abstract

A new area in which passive WiFi analytics have promise for delivering value is the real-time monitoring of public transport systems. One example is determining the true (as opposed to the published) timetable of a public transport system in real-time. In most cases, there are no other publicly-available sources for this information. Yet, it is indispensable for the real-time monitoring of public transport service levels. Furthermore, this information, if accurate and temporally fine-grained, can be used for very low-latency incident detection. In this work, we propose using spectral clustering based on trajectories derived from passive WiFi traces of users of a public transport system to infer the true timetable and two key performance indicators of the transport service, namely public transport vehicle headway and in-station dwell time. By detecting anomalous dwell times or headways, we demonstrate that a fast and accurate real-time incident-detection procedure can be obtained. The method we introduce makes use of the advantages of the high-frequency WiFi data, which provides very low-latency, universally-accessible information, while minimizing the impact of the noise in the data.

Keywords

online monitoring, incident detection, rail, machine learning

1 Introduction

WiFi access points (AP) are omnipresent and most mobile stations (cell phones, laptops, e-readers, etc.) today are equipped with WiFi functionality. In order to discover and automatically connect to known WiFi networks, mobile stations scan periodically the WiFi bands by broadcasting on all available channels so-called *probe requests* [1, 2, 3, 4]. Furthermore, even after associating successfully with an AP, mobile stations continue sending probe requests [1]. This happens especially when the connection is unstable or when user is roaming between different APs. Probe requests, specified by the IEEE 802.11 protocol [5], carry valuable information such as the MAC address of the sending device, the signal strength, etc. It is interesting to note that a mobile station's probe requests are universally accessible. While administrators of APs can simply query the system log, anyone can access probe requests sent by mobile stations using a WiFi sniffer such as `tcpdump` or `Wireshark`. Probe requests are not bound to any specific AP as they occur before the association with APs. Thus, even if no APs are present, probe requests are sent by individuals' devices and can still be observed. In addition, accessing probe requests is device-free and non-intrusive. No hardware modules are needed on the system side and no software need be installed on the individual's mobile station.

Because of these clear advantages, real-time WiFi analytics have been gaining interest among researchers in recent years. Handte *et al.* [4] designed a system to estimate the number of passengers in public transport vehicles. Musa *et al.* [1] described how to exploit probe requests to infer trajectory of vehicles by using an Hidden Markov Model (HMM). Bonné *et al.* [6] built a system on top of a Raspberry PiTM to track users' location at a mass event using probe requests, association requests and reassociation requests. Wang *et al.* [7] studied queue waiting time measurement using a single-point WiFi monitoring approach and designed queue measurement techniques adaptive to different period of time based on Bayesian networks. Manweiler *et al.* [8] designed a dwell time prediction framework in retail store environments using various sensors from smartphones including WiFi signals strength and data transmission rate. This work was extended to predict the length of stay of patrons in e.g. a retail environment using a passive WiFi sensing system and an SVM with online learning in [9].

In an offline setting, Rose *et al.* [10] leveraged probe requests to show past behaviours of users. Similarly, Cheng *et al.* [11] employed the spatial temporal information of probe requests to reveal the underlying social relationships between a small sample of users. Barbera *et al.* [3] focused on building a snapshot of thousands of users involving in a large scale event.

In addition, some companies have launched WiFi-based software products for e.g. retail shopping behavior estimation. Such products have been criticized by some to be highly error-prone and their results unstable [12]. Indeed, WiFi data are challenging to use as the sending frequency of probe requests is highly variable, depending on the mobile station’s operating system version as well as on its power management state (awake or sleeping) [1, 13, 14]. Furthermore, the observing system or AP may fail to record some probe requests because of packet loss during transmission or limited capacity of handling concurrent packets. Lastly, some MAC addresses are randomised (spoofed) in order to protect users’ privacy. It is thus very important that the applications and the methods developed to use WiFi data be robust to the above sources of noise.

While the issues raised above make WiFi-based pedestrian counting very challenging, a new area in which WiFi analytics have promise for potentially delivering great value is the real-time monitoring of public transport systems. Indeed, we shall show that some key performance indicators and real-time operational information needed for monitoring public transport systems can be obtained with remarkably high accuracy. One such example is determining the true (as opposed to the published) timetable of a public transport system in real-time. In most cases, there are no other publicly-available sources for this information. Yet, it is indispensable for the monitoring of public transport service levels. Even more importantly, this information, if accurate and temporally fine-grained, can be used for very low-latency incident detection.

In this work, we propose using spectral clustering based on trajectories derived from WiFi traces of users of a public transport system to infer the true timetable and two key performance indicators of the transport service, namely public transport vehicle headway and station dwell time. By detecting anomalous dwell times or headways, we demonstrate that a fast and accurate real-time incident-detection procedure can be obtained. The method we introduce makes use of the advantages of the high-frequency WiFi data, which provides very low-latency, universally-accessible information, while minimizing the impact of the noise in the data.

The problem of estimating or predicting the true timetable and hence delays of public transport services has been addressed in a number of research papers. For the most part, however, these papers assume access to real-time actual train locations from e.g. the train’s signaling system, or they use simulated data, or even cell phone data (voice call, SMS). In practice, though, only the train operator has access to the actual train locations and in general that data are part of a closed proprietary system which cannot be exposed in real-time for use in data analytics. In a series of papers, Kecman and Goverde use this type of data, referred to as track occupation messages, for a number of applications such as train position prediction, route conflict identification, station dwell time prediction, etc. [15, 16, 17, 18]. Similarly, [19] proposes a method to predict real-time train movements. While track occupation data are very noisy, as discussed by the authors in [16], it is nonetheless a relatively reliable source of real-time train positions. Outside the train operator itself, however, real-time track occupation data is not available.

Close in spirit to our work is the work of [20], who derive regional train timetables using large-scale cell phone data. They are able to deduce a published timetable by detecting bursts in transitions of cell phone subscribers. The authors report a precision of 85% within ± 5 minutes, but with a recall rate of only 49%. Specifically, they show that cell phone data when geo-localized against regional train stations exhibit the bursty pattern that corresponds precisely to the timetable of the regional train, and contrast that to the pattern of transitions of users geo-localized against motorway junctions, which do not show any particular pattern on the same scale. Their method works quite simply by identifying user transitions between areas within a 1km radius of a regional train station, aggregating the transitions for each station, then detecting the bursts, and associating the time of the maximum value of the burst to the train departure time. While the method works reasonably well for the highly separated regional train lines, it would not work well on an urban metro system. Indeed, the cell phone signals received by the operator are infrequent in time and have low spatial accuracy. In addition, while cell phone records can be processed by the telecommunications operator, they are not available to the general public.

Our contribution is to define a means for using passive, universally-accessible WiFi data to estimate train movements in real time. The method is based on spectral clustering of derived journeys of individual travellers in the public transport network. Our spectral clustering-based approach permits obtaining directly an estimate of each train, in space and time, without requiring apriori knowledge of the number of trains in the network. Outlier detection is critical as the WiFi data are inherently noisy; we propose a two-part outlier detection approach to handle the two main types of outliers associated with using WiFi data. The method is evaluated on data from one line of a metropolitan train (subway) system in a large city. It is shown that the results are highly accurate both during light flow conditions as well as during peak travel times in which train frequency is high and cluster separation could potentially be problematic. In addition, the method is tested on data obtained during a train disruption; it is shown that it can be effectively used for incident detection. Numerical evaluation of the method is provided against two different baselines.

The organisation of the paper is as follows. In the next section, we present the main characteristics of the WiFi data and a data aggregation method to enable use of our proposed spectral clustering approach. This includes the definition of a certain type of train journey for each passenger having a WiFi enabled device. Section 3 presents a baseline method using station-specific clustering as well as our proposed spectral clustering

method and the outlier reduction strategies developed. In Section 4 we present the evaluation of our method on WiFi data from two weeks of both peak and off-peak travel as well as during a train disruption. Section 5 concludes with a few avenues for further work in this area.

2 Preliminaries

WiFi data are obtained as a sequence of records for each device and consist of at a minimum of fields including an anonymous identifier of the device (the MAC address) as well as a timestamp and location (or in some cases a signal strength value). The update frequency of the data may be every time a probe request is sent by a device such as when a WiFi sniffer is used, or may be pre-aggregated (by an AP) to the level of e.g. each second. Recall that devices send probe requests at highly variable frequencies across the population of all devices. In some cases, one device may be recorded every second, for other devices the frequency of transmissions may be considerably less.

In order to make use of Wifi data then, it is not possible assume that lack of an observation of a particular device implies that it is no longer present. Rather, the aggregation method employed must be robust to the highly-variable frequency of observations across devices. To this end, we introduce the following notion of a *physical journey* and a τ -*journey*.

Definition 1 (physical journey). *Given a MAC address m and $\mathcal{R}_m := \{(v_i, t_i)\}_{i=1}^n$ n records associated with m . A subset $\mathcal{R}'_m \subset \mathcal{R}_m$ is called a physical journey if*

1. \mathcal{R}'_m belongs to a single train;
2. if $\mathcal{R}''_m \subset \mathcal{R}_m$ satisfies 1 and $\mathcal{R}'_m \subset \mathcal{R}''_m$, then $\mathcal{R}'_m = \mathcal{R}''_m$.

Generally, no information about the physical journey is available. Therefore we introduce the notion of a τ -*journey*, or simply *journey*, to approximate physical journey.

Definition 2 (τ -journey). *Given a MAC address m and $\mathcal{R}_m := \{(v_i, t_i)\}_{i=1}^n$ n records associated with m such that $t_1 \leq t_2 \leq \dots \leq t_n$. A subset $\mathcal{R}'_m \subset \mathcal{R}_m$ is called a τ -journey if*

1. (temporal continuity) $r_i, r_j \in \mathcal{R}'_m$ s.t. $i < j$, we have $r_k \in \mathcal{R}'_m$ for all $r_k \in \mathcal{R}_m$ such that $i < k < j$;
2. (intra-station continuity) $\max_{r_i, r_j \in \mathcal{R}'_m, v_i = v_j} |t_i - t_j| \leq \tau_1$;
3. (inter-station continuity) $\max_{r_i, r_j \in \mathcal{R}'_m, v_i \neq v_j} |t_i - t_j| \leq \tau_2$;
4. (monotonicity) $\text{sgn}((t_i - t_j)(v_i - v_j))$ is constant for all $r_i, r_j \in \mathcal{R}'_m$;
5. (maximality) if $\mathcal{R}''_m \subset \mathcal{R}_m$ satisfying 1, 2, 3 and 4 and $\mathcal{R}'_m \subset \mathcal{R}''_m$, then $\mathcal{R}'_m = \mathcal{R}''_m$.

The value of τ_1 is the average time between two *receives* of probe requests of the same device. Wang *et al.*[13] proposed values of around one or two minutes as the time between two *sends* of probe requests. Our models are more robust to the case where several actual journeys are identified as a single one than the case where one actual journeys is identified as several ones. Therefore, we choose a more conservative $\tau_1 = 8\text{min}$ as suggested in [1].

The value of τ_2 , on the other hand, depends on the train itself. Since trains may experience delays we choose a larger value such as $\tau_2 = 30\text{min}$. In general, this value should be chosen so that it is unlikely that two records of a journey are more than τ_2 minutes apart.

Figure 1 illustrates a derived journey, as defined in Definition 2. We see in particular that the device was recorded by APs not only when the owner was on his boarding and alighting station platforms but also when he/she was in the train itself, that is, when the train was in the intermediate stations during the journey. Observe further that, for a given journey, at each station, only the first and the last record at each station provide new information. Eliminating intermediate records aids in reduction of the WiFi data size by several orders of magnitude.

Figure 2 shows the average ratio of stations where a device is recorded with respect to stations at which the device actually passes, *i.e.*

$$P_{i,j} = \mathbb{E}_{\text{device } k \text{ from } i \text{ to } j} \left[\frac{\#\{\text{stations where } k \text{ is recorded}\}}{\#\{\text{stations which } k \text{ passed}\}} \right]$$

for each journey from station i to station j^* . Empirically in this example, one observes that a device is likely to be recorded at roughly 60% of stations it passes through.

We are interested in estimating the following two quantities:

*Note that the 3 main diagonals are masked since all entries are ones.

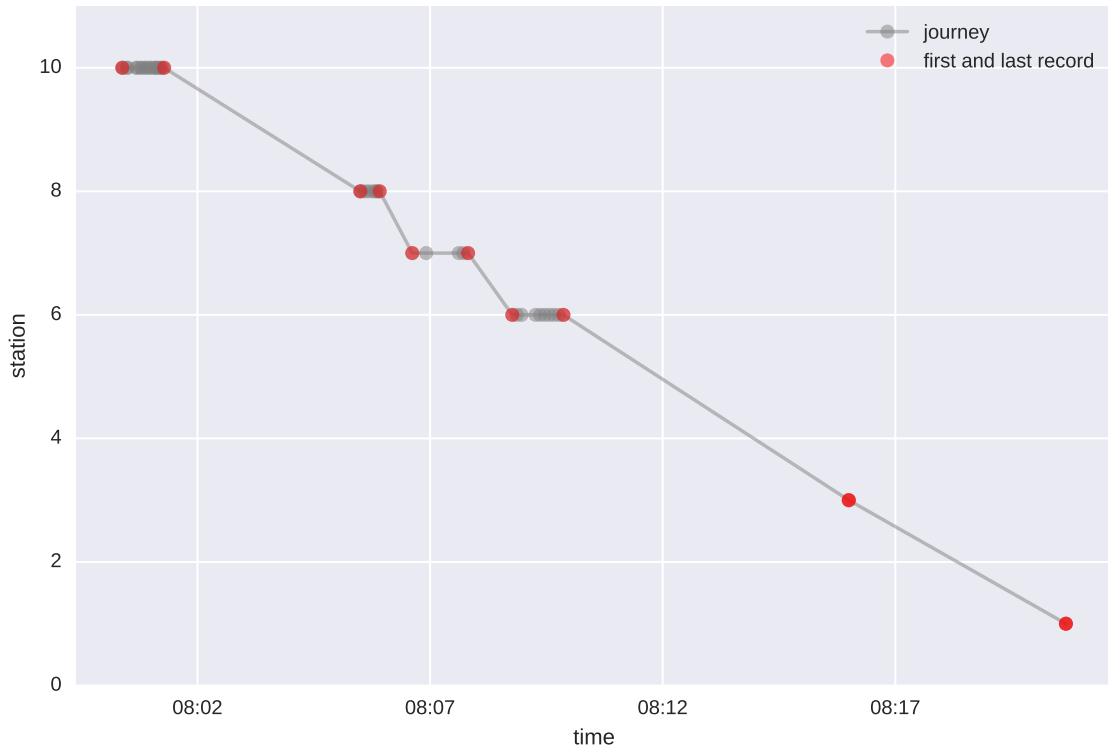


Figure 1: Example of a journey through 10 train stations with the first and the last WiFi record observed each station coloured in red.

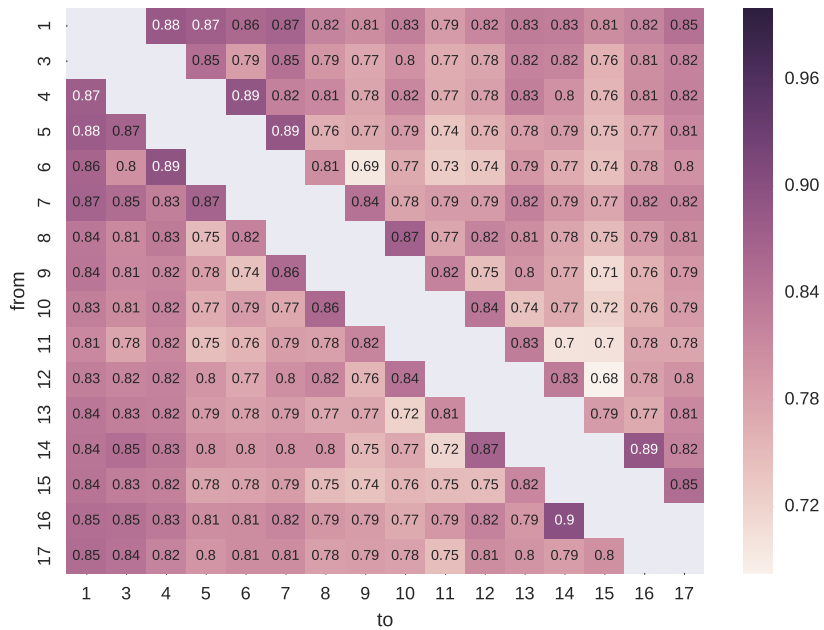
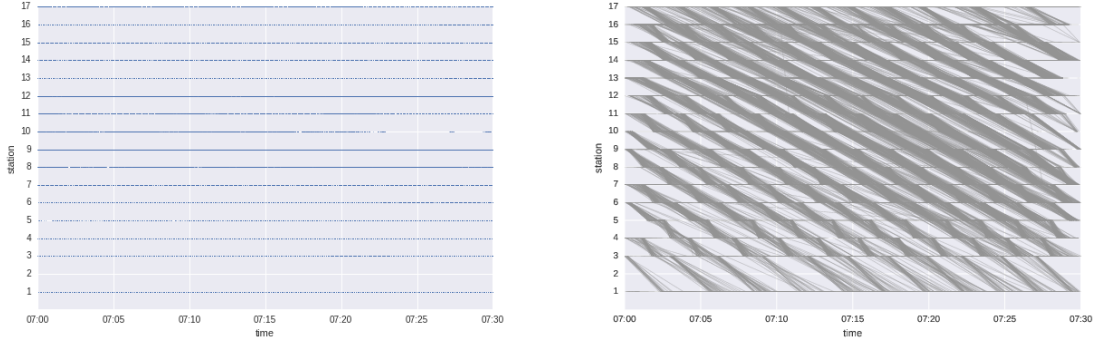


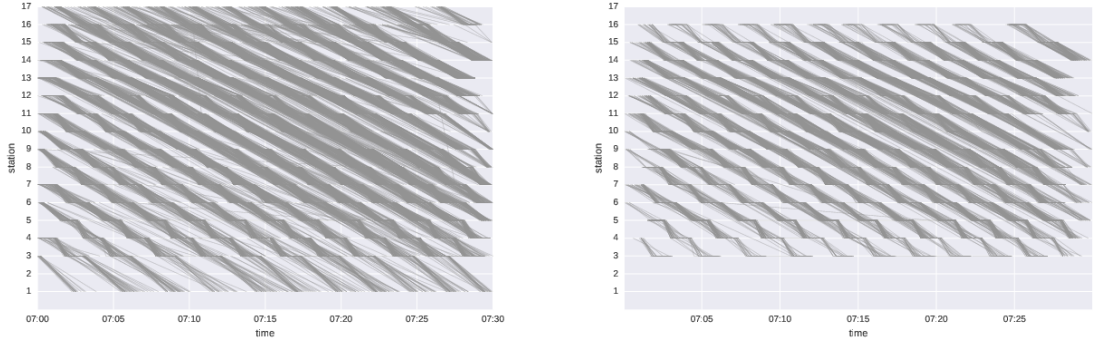
Figure 2: Heat map of average ratio of number of stations where a device is recorded

Definition 3 (Dwell time, Headway). *For a given train at a given station, we call*

- *the dwell time the time that the train stays at the station;*
- *the headway is the time difference before the departure of this train and the arrival of next train.*



(a) Raw data forming a continuum along the x axis (b) End-to-end estimated journeys. Note the high degree of noise at the boarding and alighting stations



(c) Estimated journeys where the first WiFi record at the commuter's *boarding* station and the last record at the *alighting* station were removed. (d) Estimated journeys in which all records at *boarding* and *alighting* stations were removed.

Figure 3: Data cleaning strategies for estimating individual journeys.

Deriving traveller journeys is critical for the spectral clustering method to perform well. Indeed, the WiFi data at each station, as shown in Figure 3a, form almost a continuum along the time axis at each station. Figures (3b), (3c) and (3d) show data cleaning strategies at three different levels:

- Level 1: Figure (3b) shows *all* estimated journeys according to Definition 1. Note in particular the considerable noise at the boarding and alighting stations of each journey. This is an intrinsic error associated with using WiFi data as passengers are recorded upon entry to the station and wait different amounts of time on the platform before boarding and after alighting;
- Level 2: in Figure (3c), only the last recorded observation of each device at the boarding station (and the first observation at the alighting station) and observations of all “internal” stations are used in the trajectory estimation.
- Level 3: in Figure (3d) records of boarding and alighting stations are removed. The resulting journeys are then clearly identifiable.

Using level 3 data cleaning, the first and last station of a train are lost. Thus, a hybrid strategy is employed: level 3 serves to identify trains and associate journeys to them, and level 2 serves to determine the train timetable. That is, the origin station on the line is added back once the train cluster is identified.

3 Methods

Our baseline method for determining the real-time train timetable from WiFi records involves performing 1-D clustering of timestamps at each station and then identify clusters at different stations belong to the same

train by majority vote. The method is summarized in Algorithm 1 in the Appendix. While we choose to use DBSCAN[21] in the scope of this paper, other clustering methods could also be used instead.

Figure 4 shows the result of the baseline method. Station-specific clustering, while simple and straightforward, can fail to separate two trains at one station, and as a result all subsequent stations along the line will be influenced. Consider the following example[†]: a line with three stations A, B and C and a train from A to C :

$$A \rightarrow B \rightarrow C$$

Suppose further that at station B no passengers having boarded at A are observed at B , but all passengers boarding at A and B are recognised at C . This type of anomaly can occur when e.g. a WiFi router is saturated. Algorithm 1 will consider there to be a new train at B , and errors may be introduced at station C , since some of the MAC addresses have been seen at A whereas others have been seen at B . Spectral clustering addresses this problem as it considers the trajectories of travelers and can thus readily interpolate between stations where observations are missing. Though Figure 4 appears correct, we shall see later that the baseline method fails to identify two trains.

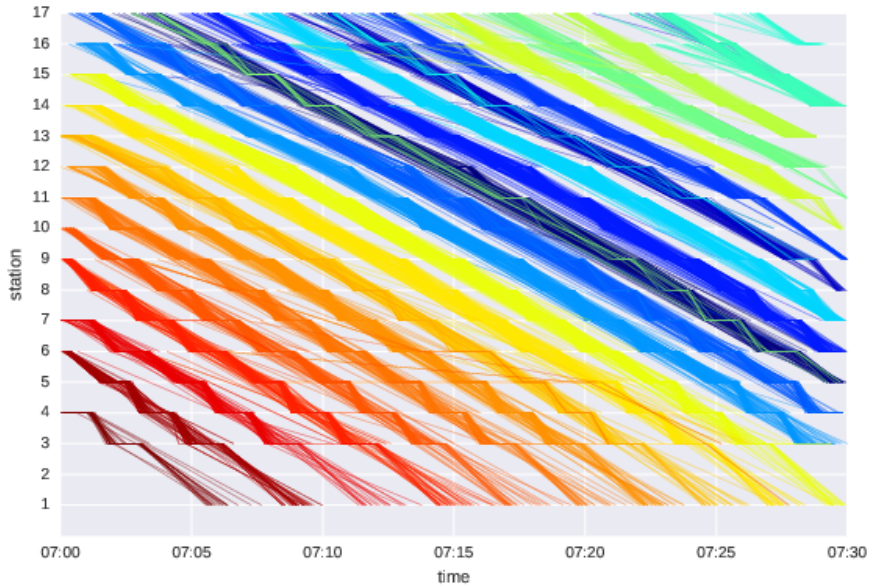


Figure 4: Clusters of figure 2 by the baseline method with $\epsilon = 6$ and $\text{min_samples} = 10$ for DBSCAN. Each colour represents a cluster label.

Spectral clustering when applied to the estimated journeys can be much more accurate than the baseline method. In addition the method is applicable to both normal and incident situations. Spectral clustering requires the definition of a similarity matrix, and uses the eigenvalues of that matrix for dimensionality reduction in the definition of the clusters. An intuitive vectorization to use is to embed a journey into $\mathbb{R}^s = \mathbb{R}^s \cup \{\infty\}$ by identifying a journey with

$$\mathbf{t} = (t_1, t_3, t_4, \dots, t_s) \quad (1)$$

where $t_k \in \mathbb{R}_+ \cup \{\infty\}$ is the mean of timestamps[‡] at stations $k = 1 \dots s$ with $t_k = \infty$ if the device is not recorded at k . In order to assess pairwise similarity, we require the following definitions:

Definition 4 (l^0 norm). Let \mathbf{t} be a point as in (1), the l^0 norm of \mathbf{t} is defined as the number of non-infinite entries of \mathbf{t} :

$$\|\mathbf{v}\|_1 = \sum_{i=1,3,4,\dots,s} \mathbb{1}_{t_i \neq \infty}.$$

Definition 5 (l^∞ norm). Let \mathbf{t} be a point as in (1), the l^∞ norm of \mathbf{t} is defined as the maximum absolute value of non-infinite entries

$$\|\mathbf{t}\|_\infty = \begin{cases} \max_{\substack{i=1,3,4,\dots,s \\ t_i \neq \infty}} |t_i|, & \text{if } \|\mathbf{v}\|_0 \neq 0, \\ \infty, & \text{otherwise.} \end{cases}$$

[†]See also figure 3a, around 07h25 at station 9.

[‡]Strictly speaking, since for a given journey, only two extremity timestamps at each station are kept, the *mean* timestamp here corresponds to the midpoint of timestamps of original data.

Definition 6 (difference). For $\mathbf{t}_1, \mathbf{t}_2$ two points as in (1), The difference of $\mathbf{t}_1, \mathbf{t}_2$ is defined as

$$\mathbf{t}_1 - \mathbf{t}_2 = (t_{1,1} - t_{2,1}, t_{1,3} - t_{2,3}, t_{1,4} - t_{2,4}, \dots, t_{1,s} - t_{2,s})$$

with $\infty - * = \infty, * - \infty = \infty$ and $\infty - \infty = \infty$.

Definition 7 (pairwise similarity). For $\mathbf{t}_1, \mathbf{t}_2$ two points as in (1), we define the following two pairwise similarity metrics:

$$\text{sim}_{\text{soft}}(\mathbf{t}_1, \mathbf{t}_2) = \|\mathbf{t}_1 - \mathbf{t}_2\|_0 \exp\left(-\frac{\|\mathbf{t}_1 - \mathbf{t}_2\|_\infty^2}{2\sigma^2}\right). \quad (2)$$

$$\text{sim}_{\text{hard}}(\mathbf{t}_1, \mathbf{t}_2) = \|\mathbf{t}_1 - \mathbf{t}_2\|_0 \mathbb{1}_{\|\mathbf{t}_1 - \mathbf{t}_2\|_\infty \leq \tau}. \quad (3)$$

Remark 8. In (2) and (3), the l^0 term quantifies the spatial similarity, i.e. number of stations where both journeys are recorded; the l^∞ term quantify the temporal similarity, i.e. maximum time difference at stations where both journeys are recorded.

Definition 9 (similarity graph). Given N points $V = \{\mathbf{t}_i\}_{i=1}^N$ as in (1), the similarity graph $\mathcal{G} = (V, E)$ is such that an edge $e_{ij} = (\mathbf{t}_i, \mathbf{t}_j)$ of weight $\text{sim}(\mathbf{t}_1, \mathbf{t}_2)$ exists if $\text{sim}(\mathbf{t}_1, \mathbf{t}_2) > 0$.

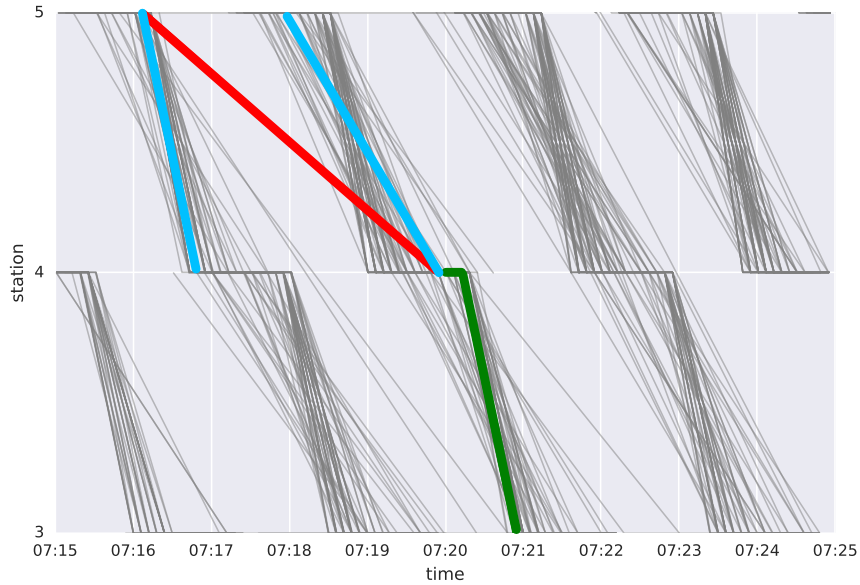


Figure 5: Behaviour of Definition 7 on mis-identified journeys. The red journey is mis-identified and is dissimilar to the two blue journeys. However, it is similar to the green journey since their timestamps at their only overlapping station are similar.

Figure 5 illustrates Definition 7 on a mis-identified journey (in red). The blue journeys are dissimilar to the red journey by the exponential in (2) and the indicator function in (3). The mis-identified journeys thus have very low degree in the similarity graph, and thus the two are unlikely to be in a single cluster using spectral clustering. Figure 6 shows the similarity graph of the estimated journeys illustrated in Figure 3d. One observes 21 well defined clusters with very few intra-cluster links.

Let $\mathcal{G} = (V, E)$ be an undirected graph with n vertices and W its weighted adjacency matrix. For a vertex $v_i \in V$, the *degree* of v_i is

$$d_i = \sum_{j=1}^n w_{i,j},$$

and the *degree matrix* D is defined as

$$D = \begin{pmatrix} d_1 & & & & \\ & d_2 & & & \\ & & \ddots & & \\ & & & d_{n-1} & \\ & & & & d_n \end{pmatrix}.$$



Figure 6: Similarity graph of data shown in Figure 3d.

Set $A \subset V$ is *connected* if any two vertices in A can be joined by a path in A . Define $i \in A$ to be $\{i|v_i \in A\}$. Then, we denote $|A|$ the number of vertices in A and $\text{vol}(A) = \sum_{i \in A} d_i$. Furthermore, for two sets $A, B \subset V$, we define

$$W(A, B) = \sum_{i \in A, j \in B} w_{i,j}.$$

Denote $\bar{A} = V - A$ the complement of A . We say A is a *connected component* if A is connected and $W(A, \bar{A}) = 0$. Non empty sets $A_1, A_2, \dots, A_k \subset V$ form a *partition* of \mathcal{G} if $A_i \cap A_j = \emptyset$ for all $i \neq j$ and $\cup_{i=1}^k A_i = V$. Denote $L = D - W$ the *non-normalised Laplacian* and $L_{rw} = D^{-1}L = I - D^{-1}W$ the *normalised Laplacian* of \mathcal{G} . We have the following result[22]:

Proposition 10. *The normalised Laplacian L_{rw} satisfies:*

- L_{rw} is positive semi-definite;
- L_{rw} has n non-negative real-valued eigenvalues $0 = \lambda_1 \leq \lambda_2 \leq \dots \leq \lambda_n$;
- the multiplicity k of eigenvalue 0 equals the number of connected components A_1, A_2, \dots, A_k of G .

Given k a number and A_1, A_2, \dots, A_k a partition of G , the *normalised Ncut* is defined as

$$\text{Ncut}(A_1, A_2, \dots, A_k) = \frac{1}{2} \sum_{i=1}^k \frac{W(A_i, \bar{A}_i)}{\text{vol}(A_i)}.$$

The minimisation of *Ncut* clearly solves the clustering problem. Further, it is worth noting that *Ncut* is robust to noise as it avoids small (and singleton) clusters. Solving *Ncut* however is NP-hard. Thus we use normalised spectral clustering (see Algorithm 2 in the Appendix) which solves a relaxation of *Ncut*.

In practice, it not easy to choose the number of clusters k *a priori*. However, as we can see from Figure 6, the similarity graph is sparse. One can use an *eigengap* heuristic[22] to determine *a priori* the optimal value of k as a function of the magnitude of the eigenvalues. Indeed, Figure 7 shows the first 30 and 40 eigenvalues of graph \mathcal{G} associated with Figure 3d; in that example, both the hard and soft similarity metrics give an eigengap around λ_{22} and λ_{25} . Algorithm 2 is extended to make use of the eigengap heuristic in Algorithm 3, also in the Appendix.

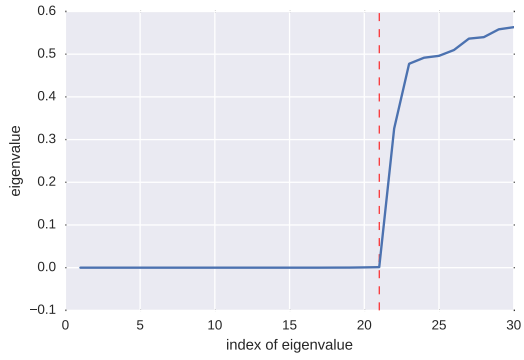
	soft similarity	hard similarity
matrix size	3047×3047	3047×3047
sparsity	91.3%	97.1%
execution time	15.1s	12.9s

Table 1: Comparison of the soft and hard similarity metrics on the estimated journeys in Figure 3d

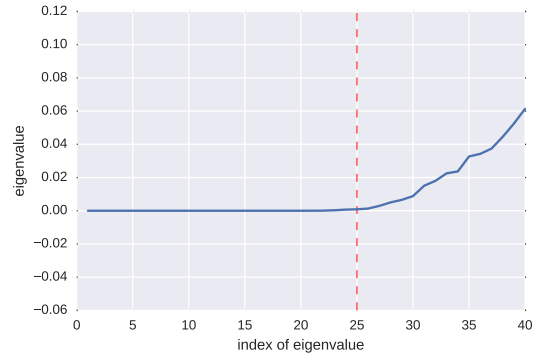
Figure 8 shows the result of spectral clustering, and Table 1 provides a comparison of the two similarity measures. One can see that the soft similarity metric fails at times to separate clusters (See for example the cluster at 7:00 at station 13 and the cluster at 7:00 at station 10).

As with the baseline method, many outliers appear in the raw result. Since it is difficult to detect those outliers *a priori*, we develop a set of two outlier detection methods, discussed next.

Figure 9 illustrates two types of anomalies in the estimated journeys arising from the use of WiFi data. The clusters are those of Figure 8a.

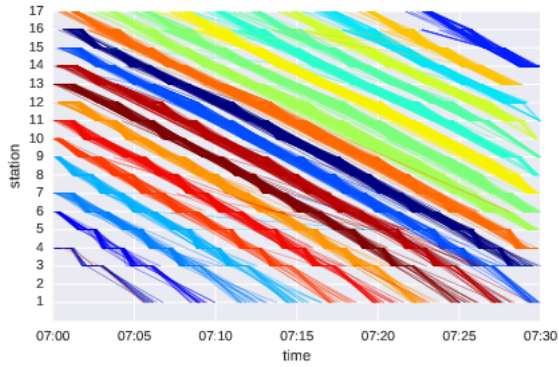


(a) Hard similarity, $\tau = 30$.

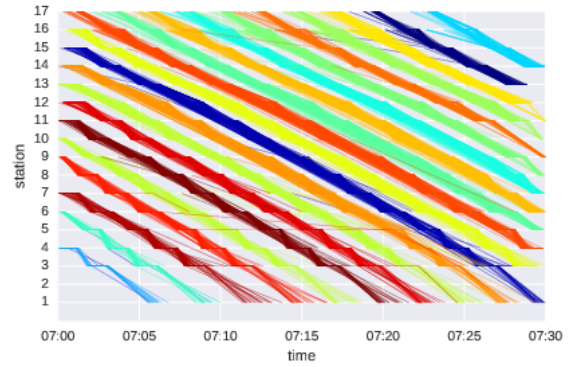


(b) Soft similarity, $2\sigma^2 = 30$.

Figure 7: First 30 eigenvalues of the normalised Laplacian of the graph associated with Figure 3d.



(a) Hard similarity, $\tau = 30$.



(b) Soft similarity, $2\sigma^2 = 30$.

Figure 8: Clusters obtained from the data of Figure 2 with the spectral clustering method. Each colour represents a cluster label.

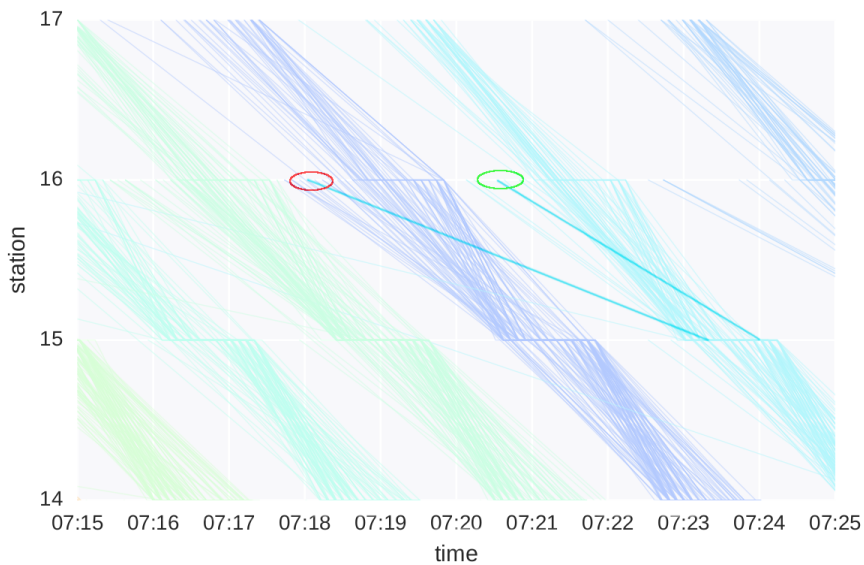


Figure 9: Two types of outliers: type 1 in red, and type 2 in green.

Type 1 outliers, shown in red in Figure 9, occur in the journey estimation step. This may represent an instance where the device owner failed to board a train but his device did not send any further probe requests while on the platform at station 16. The record highlighted in red should thus have been flagged as a separate journey.

Type 2 outliers, shown in green, can be considered intrinsic WiFi outliers as they are due to the unpredictable sending of probe requests. In this example, the last record at the boarding station or the first record at the alighting station does not match the train departure or arrival. Such WiFi records should be dropped rather than integrated into any journey.

Figure 6 shows the similarity graph of the estimated journeys in Figure 3d with vertices coloured according to cluster labels. As we can see, not all clusters are connected components: some clusters are linked together via the *type 1* outliers. The *type 2* outliers are hidden within clusters.

Type 1 Outlier Detection via k -NN *Type 1* outliers need not be isolated points in the similarity graph \mathcal{G} . While one may consider handling them by removing vertices of small degree or constructing the graph by k -nearest neighbours[22], it turns out that the connectivity of these vertices is much less predictable than that required by hard or soft threshold. A more effective approach to handling *Type 1* outliers is after the spectral clustering step.

Reexamining Figures 8a and 6, note that the *Type 1* outliers are such that the journey’s cluster label is different from the lab of its k nearest neighbours at that station. Thus the method developed for *Type 1* outlier removal is through a k -NN approach; see Algorithm 4 in the Appendix. The k -NN is not only robust to mis-classified journeys, but also to a having too many clusters k .

Type 2 Outlier Detection via a Mean-Absolute-Deviation Distance Metric *Type 2* outliers cannot be readily identified by k -NN. Hence, a more traditional method was developed to detect these outliers.

Definition 11 (Median absolute deviation). *Let $x_1, x_2, \dots, x_n \in \mathbb{R}$, the median absolute deviation is defined as*

$$\text{MAD} = \text{median}_{i=1}^n(x_i - \text{median}_{j=1}^n x_j).$$

Definition 12 (Consistent estimator of standard deviation). *Let $x_1, x_2, \dots, x_n \sim \mathcal{N}(\mu, \sigma)$ i.i.d and MAD the median absolute deviation, then*

$$\hat{\sigma} = \frac{1}{\Phi^{-1}(3/4)} \text{MAD} \approx 1.4826 \text{ MAD}$$

is a consistent estimator of σ [23].

The advantage of using Definition 12 as the estimator of standard deviation is that it is robust to outliers as long as they are a minority. Algorithm 5 in the Appendix was developed using these two definitions for *Type 2* outlier detection.

The clusters that result from the spectral clustering step after outlier removal represent the space-time trajectories of each train. For each cluster and every station, the arrival and departure times are given by the minimum and maximum timestamps in the cluster. To estimate trains when intermediate stations have no WiFi observations, the envelope (not necessarily convex) of each cluster can be used to connect the arrival and departure times at stations with data.

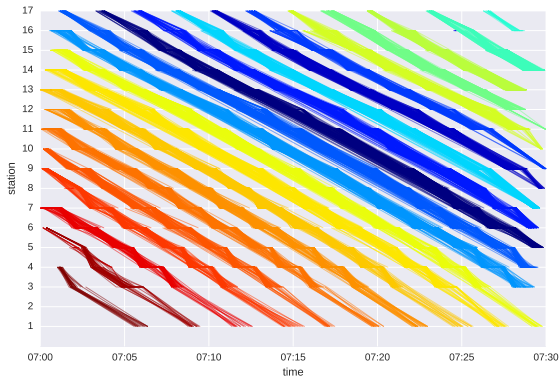
4 Quantitative Evaluation

The Figures 10 illustrate a comparison of the baseline method versus the proposed spectral clustering approach. The figures show the resulting clusters and the estimated train trajectories from the envelope using the two methods. Despite outlier detection, the baseline method fails to merge two clusters to their corresponding trains. Neglecting the boundary effect[§] at lower-left and upper-right corner of figure 10d into account, the spectral clustering gives the correct number of trains.

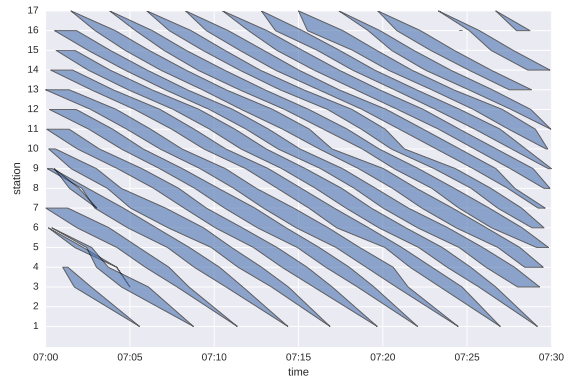
To quantitatively evaluate the performance of the methods, we compare the result using both the baseline method and the spectral clustering approach with manual counts of the train arrival times obtained over a period of several hours during peak travel times at four stations over the five workdays during one week. The results are evaluated quantitatively using the following metrics:

- number of trains;
- number of hits, *i.e.* number of trains whose error to ground survey is within ± 1 minute;

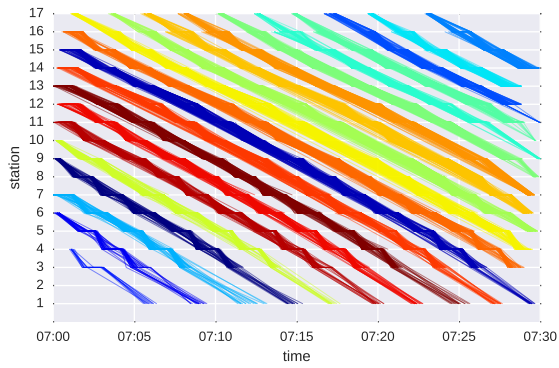
[§]In practice, it suffice to partition the data into overlapped time slots to handle this boundary effect.



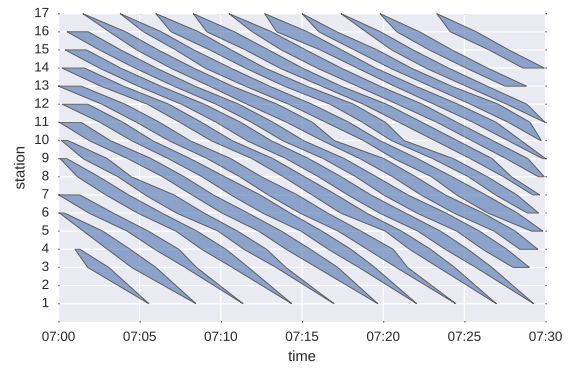
(a) Clusters with outliers removed by baseline



(b) Envelope of trains' arrival and departure point by baseline



(c) Clusters with outliers removed by spectral clustering



(d) Envelope of trains' arrival and departure point by spectral clustering

Figure 10: Clusters and trains' arrival and departure by the baseline method and the spectral clustering. Outlier handling is performed using Algorithms 4 and 5.

- hit rate, *i.e.* number of hits / number of trains;
- Root mean squared error (RMSE) of train arrival time (in minutes).

Note that the last three quantities can only be calculated when the number of trains is the same as that of the manual counts.

Venue	Manual counts		Baseline		Spectral Clustering	
	mean	std	mean	std	mean	std
6	40.67	0.58	12.00	1.73	40.33	0.58
8	12.20	5.72	42.60	5.73	42.20	5.72
10	43.75	3.77	44.50	2.89	44.00	3.46
12	42.70	5.17	44.40	5.62	42.40	5.50
13	47.00	0.00	47.33	0.58	47.00	0.00
15	46.00	0.00	45.50	0.71	45.50	0.71

Table 2: Comparison of number of trains of the baseline method and spectral clustering.

Venue	Baseline		Spectral Clustering	
	mean	std	mean	std
6	0.63	NaN	0.89	0.09
8	0.68	0.54	0.85	0.21
10	0.59	0.53	0.72	0.44
12	0.77	0.23	0.88	0.19
13	1.00	0.00	1.00	0.00
15	1.00	NaN	1.00	0.00

Table 3: Comparison of hit rate of the baseline method and spectral clustering.

Venue	Baseline		Spectral Clustering	
	mean	std	mean	std
6	1.23	NaN	0.51	0.40
8	2.55	4.29	0.88	1.55
10	0.71	0.72	0.53	0.60
12	0.46	0.34	0.26	0.25
13	0.00	0.00	0.00	0.00
15	0.00	NaN	0.00	NaN

Table 4: Comparison of RMSE of the baseline method and spectral clustering.

Tables 2, 3 and 4 show the mean number of trains observed manually, and the mean number of trains estimated by the baseline method and our proposed spectral clustering approach.

One flaw of the baseline method is that it is prone to “inventing” trains by creating clusters that do not correspond to any physical train. The spectral clustering approach, as it considers journeys, does not suffer from this problem. Tables 3 and 4 show a comparison of the hit rate and RMSE of both methods. The spectral clustering approach is empirically more stable and outperforms the baseline method in terms of both hit rate and RMSE.

To assess the performance of the models during a train disruption, we run the models on the WiFi data obtained during a two-hour train incident. Specifically, a train disruption occurred at station 15 between 7 and 8 am wherein the traffic was interrupted for half an hour and then partially resumed but remained perturbed until 9am. Shortly after the incident, shuttle buses were put into service to help commuters to “skip” the affected station 15. Figure 11 shows the derived journeys. Table 5 shows a comparison of the baseline method and the spectral clustering approach. The spectral clustering approach again outperforms the baseline both in terms of hit rate and RMSE.

Figure 12 shows how such a system can be used for very low-latency incident detection in real-time in the public transport network. The figure shows a time series of the derived train headways at station 15 produced by the spectral clustering approach during the incident period. The headways are derived from the estimated timetable as simply taking the difference between successive arrivals of the trains into the station. The sharp increase in headway is evident in the peaks shortly after the incident occurs.

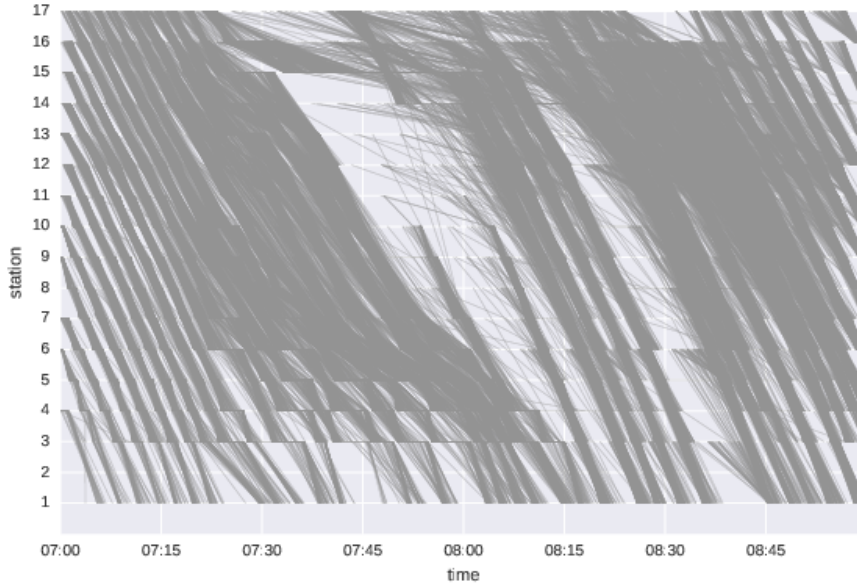


Figure 11: Derived journeys during an incident.

Venue	Number of Trains			Hit rate		RMSE	
	Manual counts	Baseline	Spectral	Baseline	Spectral	Baseline	Spectral
8	33	33	33	0.06	0.52	7.50	3.63
12	30	30	29	0.66	-	0.84	-

Table 5: Comparison of number of trains, hit rate and RMSE of the baseline method and spectral clustering to ground survey during an incident period.

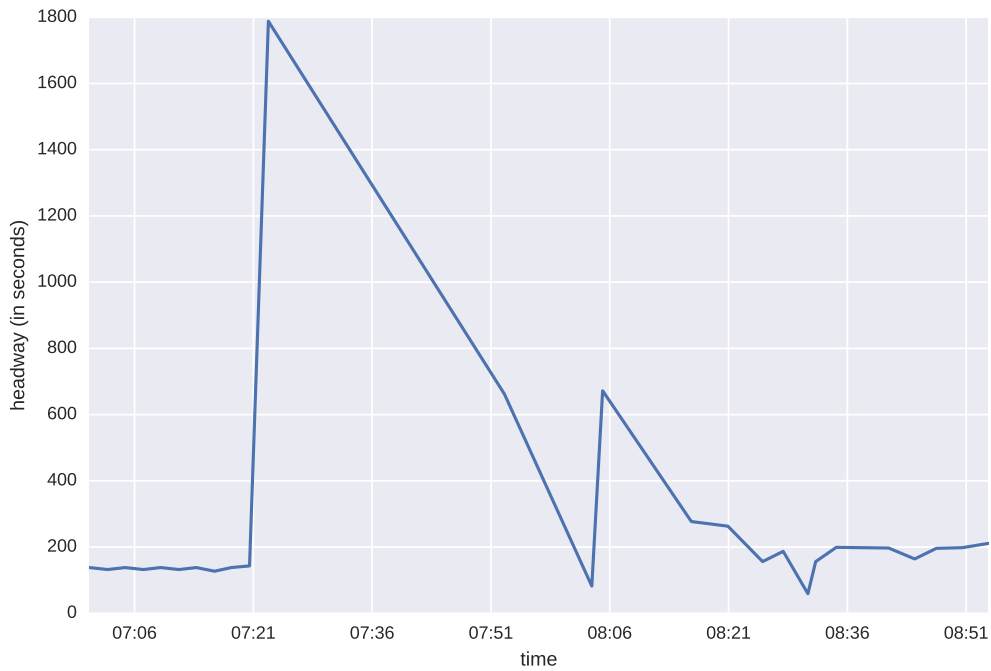


Figure 12: Headways at station 15 derived from the estimated timetable obtained through the spectral clustering approach during an incident period.

5 Conclusions

We have presented a passive WiFi based approach to monitor public transport service levels in real-time. Specifically, we propose a spectral clustering method based on derived commuter trajectories to determine the real-time train timetable, and thus the actual train headways and in-station dwell times. In most cases, there are no other publicly-available sources for this information. Yet, it is indispensable for the real-time monitoring of public transport service levels such as train delays. We showed how the proposed system can be used for very low-latency incident detection in the public transport system by detecting anomalous headways or in-station dwell times. The methods proposed make use of the advantages of the high-frequency WiFi data while minimizing the impact of the noise in the data.

We considered each line of the train network separately and derived the values of interest by train line. It would be of interest to extend the methodology to handle journeys across multiple lines, i.e. with transfers, as well as multi-modal journeys, if WiFi traces can be retrieved, e.g. from bus stops as well as the train stations. A natural extension of this work is also for the monitoring of crowd-related public transport service levels and disruptions. However, the noise inherent in the passive WiFi data are more challenging as regards the estimation of crowd-related quantities.

Acknowledgments

The authors gratefully acknowledge the contribution of the Singapore Land Transport Authority (LTA) to the work described in this paper.

References

- [1] A. B. M. Musa and Jakob Eriksson. Tracking unmodified smartphones using wi-fi monitors. In *Proceedings of the 10th ACM Conference on Embedded Network Sensor Systems*, SenSys '12, pages 281–294, New York, NY, USA, 2012. ACM.
- [2] Mathieu Cunche. Smartphone, Wi-Fi et vie privée : comment votre smartphone peut se révéler être votre pire ennemi, October 2013. 1.
- [3] Marco V. Barbera, Alessandro Epasto, Alessandro Mei, Vasile C. Perta, and Julinda Stefa. Signals from the crowd: Uncovering social relationships through smartphone probes. In *Proceedings of the 2013 Conference on Internet Measurement Conference*, IMC '13, pages 265–276, New York, NY, USA, 2013. ACM.
- [4] Marcus Handte, Muhammad Umer Iqbal, Stephan Wagner, Wolfgang Apolinarski, Pedro José Marrón, Eva Maria Muñoz Navarro, Santiago Martinez, Sara Izquierdo Barthelemy, and Mario González Fernández. Crowd Density Estimation for Public Transport Vehicles. In *Workshop Proceedings of the EDBT/ICDT 2014 Joint Conference*, 2014.
- [5] IEEE Computer Society. IEEE 802.11: Wireless LAN Medium Access Control (MAC) and Physical Layer (PHY) Specifications, 2012.
- [6] B. Bonné, A. Barzan, P. Quax, and W. Lamotte. Wifipi: Involuntary tracking of visitors at mass events. In *World of Wireless, Mobile and Multimedia Networks (WoWMoM), 2013 IEEE 14th International Symposium and Workshops on a*, pages 1–6, June 2013.
- [7] Yan Wang, Jie Yang, Yingying Chen, Hongbo Liu, Marco Gruteser, and Richard P. Martin. Tracking human queues using single-point signal monitoring. In *Proceedings of the 12th Annual International Conference on Mobile Systems, Applications, and Services*, MobiSys '14, pages 42–54, New York, NY, USA, 2014. ACM.
- [8] J. Manweiler, N. Santhapuri, R. R. Choudhury, and S. Nelakuditi. Predicting length of stay at wifi hotspots. In *INFOCOM, 2013 Proceedings IEEE*, pages 3102–3110, April 2013.
- [9] Viet Le Truc, Baoyang Song, and Laura Wynter. Real-time prediction of length of stay using passive wi-fi sensing, 2016. submitted.
- [10] Ian Rose and Matt Welsh. Mapping the urban wireless landscape with argos. In *Proceedings of the 8th ACM Conference on Embedded Networked Sensor Systems*, SenSys '10, pages 323–336, New York, NY, USA, 2010. ACM.
- [11] N. Cheng, P. Mohapatra, M. Cunche, M. A. Kaafar, R. Boreli, and S. Krishnamurthy. Inferring user relationship from hidden information in wlans. In *MILCOM 2012 - 2012 IEEE Military Communications Conference*, pages 1–6, Oct 2012.

- [12] Fiona Manzella and Iris Ten-Teije. The truth about in-store analytics: Examining wi-fi, bluetooth and video in retail, 2015.
- [13] Wei Wang, Raj Joshi, Aditya Kulkarni, Wai Kay Leong, and Ben Leong. Feasibility study of mobile phone wifi detection in aerial search and rescue operations. In *Proceedings of the 4th Asia-Pacific Workshop on Systems*, APSys '13, pages 7:1–7:6, New York, NY, USA, 2013. ACM.
- [14] Loh Chin Choong Desmond, Cho Chia Yuan, Tan Chung Pheng, and Ri Seng Lee. Identifying unique devices through wireless fingerprinting. In *Proceedings of the First ACM Conference on Wireless Network Security*, WiSec '08, pages 46–55, New York, NY, USA, 2008. ACM.
- [15] Pavle Kecman and Rob MP Goverde. An online railway traffic prediction model. In *RailCopenhagen2013: 5th International Conference on Railway Operations Modelling and Analysis, Copenhagen, Denmark, 13-15 May 2013*. International Association of Railway Operations Research (IAROR), 2013.
- [16] P Kecman and RMP Goverde. Process mining of train describer event data and automatic conflict identification. *Computers in railways XIII, WIT transactions on the built environment*, 127:227–238, 2013.
- [17] Pavle Kecman and Rob MP Goverde. Online data-driven adaptive prediction of train event times. *IEEE Transactions on Intelligent Transportation Systems*, 16(1):465–474, 2015.
- [18] Pavle Kecman and Rob MP Goverde. Predictive modelling of running and dwell times in railway traffic. *Public Transport*, 7(3):295–319, 2015.
- [19] Luke J. W. Martin. *Predictive Reasoning and Machine Learning for the Enhancement of Reliability in Railway Systems*, pages 178–188. Springer International Publishing, Cham, 2016.
- [20] Christopher Horn and Roman Kern. Deriving public transportation timetables with large-scale cell phone data. *Procedia Computer Science*, 52:67 – 74, 2015.
- [21] Martin Ester, Hans peter Kriegel, Jörg Sander, and Xiaowei Xu. A Density-Based Algorithm for Discovering Clusters in Large Spatial Databases with Noise. In *Knowledge Discovery and Data Mining*, pages 226–231, 1996.
- [22] Ulrike von Luxburg. A tutorial on spectral clustering. *Statistics and Computing*, 17(4):395–416, 2007.
- [23] Peter J. Rousseeuw and Christophe Croux. Alternatives to the median absolute deviation. *Journal of the American Statistical Association*, 88(424):1273–1283, 1993.

A Appendix

Algorithm 1: Baseline method

```
input : Set of  $N$  records  $\mathcal{R} = \{(m_i, v_i, t_i)\}_{i=1}^N$  with  $m_i$  MAC address,  $v_i$  venue id and  $t_i$  timestamp
1 for every venue id  $v$  in  $\mathcal{R}$  do
2   set of clusters  $\mathcal{C}_v = \{C_{v,-1}, C_{v,0}, C_{v,1}, \dots, C_{v,n}\} \leftarrow$  DBSCAN
3   remove  $C_{v,-1}$  // DBSCAN gives outliers the label  $-1$ 
4   for every cluster  $C_{v,i}$  do
5     old_labels =  $\emptyset$ 
6     for every record  $r_{v,i,k}$  in  $C_{v,i}$  do
7       if exists  $r_{v',i',k'} = r_{v,i,k}$  s.t. the difference of timestamps falls in  $[\tau_1, \tau_2]$  then
8         |  $i_{\text{old}} = i'$ 
9       else
10        |  $i_{\text{old}} = -1$ 
11        | append  $i_{\text{old}}$  to old_labels
12    take old_label as the majority of old_labels
13    // the cluster correspond to a train seen previously
14    if old_label  $\neq -1$  then
15      | change the label of  $C_{v,i}$  to old_label
16      // the cluster stands for a new train
17    else
18      | change the label of  $C_{v,i}$  to  $\max\{i|C_{v,i}\} + 1$ 
```

Algorithm 2: Normalised spectral clustering[22]

```
input : Set of  $N$  points  $V = \{t_i\}_{i=1}^N$ 
        Number of clusters  $k$ 
         $\tau$  for  $\text{sim}_{\text{hard}}$  or  $\sigma$  for  $\text{sim}_{\text{soft}}$ 
1 Construct graph  $\mathcal{G}$  with weight matrix  $W$  as in definition 9
2 Remove all isolated points
3 Compute the unnormalized Laplacian  $L$ 
4 Compute the eigenvalues and eigenvalues of generalized eigenproblem  $Lu = \lambda Du$ 
5 Keep only the first  $k$  eigenvectors  $u_1, \dots, u_k$ 
6 Let  $U \in \mathbb{R}^{N \times k}$  be the matrix containing  $u_1, \dots, u_k$  as columns
7 For  $i = 1, \dots, n$ , let  $y_i \in \mathbb{R}^k$  be the vector corresponding to the  $i$ -th row of  $U$ 
8 Cluster the points  $(y_i)_{i=1, \dots, n}$  in  $\mathbb{R}^k$  with the  $k$ -means algorithm into  $k$  clusters
output:  $N$  labels  $\{l_i\}_{i=1}^N \subset \llbracket 1, k \rrbracket^N$ 
```

Algorithm 3: Normalised spectral clustering with adaptive number of clusters

```
input : Set of  $N$  points  $V = \{t_i\}_{i=1}^N$ 
         $\tau$  for  $\text{sim}_{\text{hard}}$  or  $\sigma$  for  $\text{sim}_{\text{soft}}$ 
1 Construct graph  $\mathcal{G}$  with weight matrix  $W$  as in definition 9
2 Remove all isolated points
3 Compute the unnormalized Laplacian  $L$ 
4 Compute the eigenvalues and eigenvalues of generalized eigenproblem  $Lu = \lambda Du$ 
5 Choose the number of clusters  $k$  by eigengap heuristic
6 Keep only the first  $k$  eigenvectors  $u_1, \dots, u_k$ 
7 Let  $U \in \mathbb{R}^{N \times k}$  be the matrix containing  $u_1, \dots, u_k$  as columns
8 For  $i = 1, \dots, n$ , let  $y_i \in \mathbb{R}^k$  be the vector corresponding to the  $i$ -th row of  $U$ 
9 Cluster the points  $(y_i)_{i=1, \dots, n}$  in  $\mathbb{R}^k$  with the  $k$ -means algorithm into  $k$  clusters
output:  $N$  labels  $\{l_i\}_{i=1}^N \subset \llbracket 1, k \rrbracket^N$ 
```

Algorithm 4: Type 1 outlier detection using k -NN

input : N records $\mathcal{R} = \{r_i\}_{i=1}^N = \{(m_i, v_i, t_i, c_i)\}_{i=1}^N$ with m_i MAC address, v_i venue id, t_i timestamp and c_i cluster label;
number of neighbours k

- 1 **for** every venue id v in \mathcal{R} **do**
- 2 $\mathcal{R}_v \leftarrow \{r_i \in \mathcal{R} | v_i = v\}$
- 3 use k -NN to assign a new cluster label $c_v^{\text{neighbour}}$ to every record r_v
- 4 $\mathcal{R}' \leftarrow \{r_i \in \mathcal{R} | c_i = c_i^{\text{neighbour}}\}$

output: \mathcal{R}'

Algorithm 5: Type 2 outlier detection using Median Absolute Deviation

input : N records $\mathcal{R} = \{r_i\}_{i=1}^N = \{(m_i, v_i, t_i, c_i)\}_{i=1}^N$ with m_i MAC address, v_i venue id, t_i timestamp and c_i cluster label;
threshold τ

- 1 **for** every venue id v in \mathcal{R} **do**
- 2 $\mathcal{R}_v \leftarrow \{r_i \in \mathcal{R} | v_i = v\}$
- 3 **for** every label c **do**
- 4 $\mathcal{R}_{v,c} \leftarrow \{r_i \in \mathcal{R}_v | c_i = c\}$
- 5 $MAD \leftarrow \text{MAD}(t_{v,c})$
- 6 $\hat{\sigma} = 1.4826MAD$
- 7 **for** every label $r_{v,c}$ **do**
- 8 **if** $|t_{v,c} - MAD| \geq \tau \hat{\sigma}$ **then**
- 9 remove $r_{v,c}$

output: \mathcal{R}'
